Journal of Experimental Botany, Vol. 63, No. 17, pp. 6237–6251, 2012
doi:10.1093/jxb/ers279
This paper is available online free of all access charges (see http://jxb.oxfordjournals.org/open_access.html for further details)

Journal of Experimental Botany
www.jxb.oxfordjournals.org

RESEARCH PAPER

Proteomic analysis of grapevine resistance induced by *Trichoderma harzianum* T39 reveals specific defence pathways activated against downy mildew

Maria Cristina Palmieri[1], Michele Perazzolli[1,*], Vittoria Matafora[2], Marco Moretto[1], Angela Bachi[2] and Ilaria Pertot[1]

[1] IASMA Research and Innovation Centre, Fondazione Edmund Mach, via E. Mach 1, 38010 San Michele all'Adige, Trento, Italy
[2] Biological Mass Spectrometry Unit DIBIT, San Raffaele Scientific Institute, via Olgettina 58, 20132 Milano, Italy

* To whom correspondence should be addressed. E-mail: michele.perazzolli@fmach.it

Received 7 June 2012; Revised 15 August 2012; Accepted 11 September 2012

Abstract

Downy mildew is caused by the oomycete *Plasmopara viticola* and is one of the most serious diseases of grapevine. The beneficial microorganism *Trichoderma harzianum* T39 (T39) has previously been shown to induce plant-mediated resistance and to reduce the severity of downy mildew in susceptible grapevines. In order to better understand the cellular processes associated with T39-induced resistance, the proteomic and histochemical changes activated by T39 in grapevine were investigated before and 1 day after *P. viticola* inoculation. A comprehensive proteomic analysis of T39-induced resistance in grapevine was performed using an eight-plex iTRAQ protocol, resulting in the identification and quantification of a total of 800 proteins. Most of the proteins directly affected by T39 were found to be involved in signal transduction, indicating activation of a complete microbial recognition machinery. Moreover, T39-induced resistance was associated with rapid accumulation of reactive oxygen species and callose at infection sites, as well as changes in abundance of proteins involved in response to stress and redox balance, indicating an active defence response to downy mildew. On the other hand, proteins affected by *P. viticola* in control plants mainly decreased in abundance, possibly reflecting the establishment of a compatible interaction. Finally, the high-throughput iTRAQ protocol allowed *de novo* peptide sequencing, which will be used to improve annotation of the *Vitis vinifera* cv. Pinot Noir proteome.

Key words: biocontrol agent, induced resistance, *Plasmopara viticola*, quantitative proteomics, reactive oxygen species, tripartite interaction, *Vitis vinifera*.

Introduction

The oomycete *Plasmopara viticola* (Berk. & Curt.) Berl. & de Toni is the causal agent of downy mildew, one of the most damaging diseases of grapevine. *P. viticola* is an obligate biotroph, which infects leaves and clusters of young berries. To acquire nutrients, it penetrates into the substomatal cavity where the primary hyphae develop and then expand to form complex intercellular mycelia with haustoria within host mesophyll cells (Unger *et al.*, 2007; Díez-Navajas *et al.*, 2008).

Resistant *Vitis* species exhibit varying levels of resistance and *P. viticola* infection may be obstructed by an array of plant responses (Gessler *et al.*, 2011). Aside from constitutive physical and chemical barriers, downy mildew resistance is mainly based on post-infection processes (Díez-Navajas *et al.*, 2008; Polesani *et al.*, 2010). Microscopic observations have revealed that the first stages of infection are essentially the same in both susceptible and resistant grapevines, and development of the

disease is restricted after the first haustoria have established contact with the mesophyll cells (Unger *et al.*, 2007; Diez-Navajas *et al.*, 2008; Polesani *et al.*, 2010). Post-infection mechanisms include fortification of plant cell walls through localized callose deposition (Diez-Navajas *et al.*, 2008; Jürges *et al.*, 2009), coupled with generation of reactive oxygen species (ROS), increase in peroxidase activity and hypersensitive response activation (Kortekamp, 2006; Diez-Navajas *et al.*, 2008).

The susceptibility of *Vitis vinifera* to downy mildew suggests that this species lacks a *P. viticola*-specific recognition system (Di Gaspero *et al.*, 2007). However, transcriptional (Hamiduzzaman *et al.*, 2005; Kortekamp, 2006; Trouvelot *et al.*, 2008; Polesani *et al.*, 2010) and proteomic (Milli *et al.*, 2011) changes associated with the early stages of *P. viticola* infection indicate the presence of a weak, but insufficient, defence response in susceptible grapevines.

Several substances with the ability to activate plant-mediated defence mechanisms and increase grapevine resistance to downy mildew have been identified (Hamiduzzaman *et al.*, 2005; Trouvelot *et al.*, 2008). For example, benzothiadiazole-7-carbothioic acid S-methyl ester (BTH) has been found to significantly reduce downy mildew symptoms in susceptible grapevines (Perazzolli *et al.*, 2008) by activating salicylic acid (SA)-dependent pathways, with a high energy cost for the plant (Perazzolli *et al.*, 2011). In addition to chemical inducers, some beneficial soil-borne microorganisms have been shown to promote plant growth and activate induced systemic resistance against a broad spectrum of pathogens and insects (Van Hulten *et al.*, 2010). In particular, *Trichoderma* spp. are ubiquitous filamentous fungi that colonize the rhizosphere and phyllosphere, promote plant growth, and antagonize numerous foliar and root pathogens (Vinale *et al.*, 2008; Shoresh *et al.*, 2010). *Trichoderma* spp. have various antagonistic mechanisms, including competition for nutrients and space, production of antifungal compounds, direct parasitism, and induction of plant resistance (Vinale *et al.*, 2008; Shoresh *et al.*, 2010) by reprogramming the plant transcriptome (Bailey *et al.*, 2006; Alfano *et al.*, 2007; Brotman *et al.*, 2012; Morán-Diez *et al.*, 2012) and proteome (Segarra *et al.*, 2007; Shoresh and Harman, 2008). Treatments with *Trichoderma harzianum* T39 (T39) has been found to activate grapevine resistance to downy mildew (Perazzolli *et al.*, 2008) without negative effects on plant growth (Perazzolli *et al.*, 2011). Although T39 appears to be a promising alternative for controlling downy mildew in the vineyard, the key components of the defence mechanism need to be identified in order to better understand how this method of biocontrol functions and how to maximize its efficacy.

This study analysed proteomic changes occurring in grapevine leaves in response to T39 treatment and *P. viticola* inoculation using the high-throughput eight-plex iTRAQ protocol in order to identify proteins and pathways affected by resistance activation. A histological analysis of cellular responses to *P. viticola* inoculation was carried out in order to clarify cellular processes of T39-induced resistance.

Materials and methods

Resistance induction and assessment of disease in grapevine plants

Susceptible grapevine *V. vinifera* cv. Pinot Noir plants and the *P. viticola* inoculum were grown and propagated as previously described in Perazzolli *et al.* (2008). A commercial product based on *T. harzianum* T39 (Trichodex, Makhteshim, Israel) was applied at a concentration of 8 g l^{-1} in water, corresponding to a conidia suspension of approximately 10^5 colony-forming units ml^{-1}. In addition, plants were either treated with water (control) or with the chemical inducer BTH (Bion 50WG, Syngenta Crop Protection, Switzerland) diluted in water at a concentration of 0.5 g l^{-1}. The abaxial and adaxial surfaces of all the leaves of the grapevine plants were sprayed three times with T39, BTH, or water (20–30 ml per plant, depending on the number of leaves) using a compressed air hand sprayer, avoiding any spilling or dripping. Treatments were carried out at 3, 2, and 1 days before pathogen inoculation. One day after the final treatment, a fresh suspension of *P. viticola* sporangia (10^5 sporangia ml^{-1}) was sprayed onto the abaxial leaf surfaces of all grapevine leaves (20–30 ml per plant, depending on the number of leaves). Inoculated plants were incubated overnight in the dark at 25 °C and 99–100% relative humidity and then kept under controlled greenhouse conditions. Ten days after inoculation, plants were incubated overnight in the dark at 25 °C and 99–100% relative humidity. Disease severity was visually assessed as the percentage of the abaxial leaf surface area covered by sporulation, and disease incidence was calculated as the percentage of leaves showing sporulation (EPPO, 2001). Twelve plants (replicates) were analysed for each treatment in a randomized complete block, and the experiment was carried out three times.

Resistance induction and assessment of disease in grapevine leaf discs

The third and fourth leaves from the top of the plants were collected and washed in tubes containing a 1% hypochlorite solution for 10 min (Sánchez Márquez *et al.*, 2007). After treatment they were rinsed three times in sterile water. Leaf discs with a diameter of 1 cm were then cut and transferred (lower surface uppermost) onto moist filter paper (three foils) in Petri dishes (9 cm diameter). A total of 45 discs were prepared: 15 discs per treatment placed in each of three Petri dishes. A Potter Precision Spray Tower (Burkard Scientific, UK) was used to spray 1.5 ml water suspension onto each Petri dish at a pressure of 48.2 MPa. Water, T39, and BTH were applied at 3, 2, and 1 days before pathogen inoculation. After each treatment the discs were left to dry and then kept at 25 °C under greenhouse conditions. One day after the final treatment, leaf discs were spayed (1.5 ml per dish) with a fresh suspension of *P. viticola* (10^5 sporangia ml^{-1}), then immediately covered and kept at 25 °C under greenhouse conditions. Seven days after inoculation, the percentage of disc area covered by downy mildew sporulation was visually assessed.

For treatment with the inhibitor of callose synthesis, leaf discs were floated on a solution of 2 mM 2-deoxy-D-glucose (2-DDG, Sigma-Aldrich, MO) in water for 24 h in the dark (Bayles *et al.*, 1990), while control leaf discs were floated on water for 24 h in the dark. The leaf discs were then washed twice in water and transferred to Petri dishes (lower surface uppermost) for subsequent treatments with water, T39, or BTH followed by *P. viticola* inoculation, as described above.

Aniline blue staining

In order to observe *P. viticola* structures and callose deposition in plant cells, leaf discs were collected before inoculation (uninoculated) and at 1, 5, and 7 days post inoculation (dpi) with *P. viticola* then stained with aniline blue (Sigma-Aldrich) according to Díez-Navajas *et al.* (2007). The discs were then incubated in 0.05% aniline blue in 0.067 M K_2HPO_4 pH 8. Microscope observations

were carried out with a Leica LMD7000 microscope (Germany) using two different excitation filters: an A4 filter (BP 320–400 nm excitation, 400 nm dichroic mirror, and BP 470 nm emission) for blue-based images and an H3 filter (BP 420–490 nm excitation, 510 nm dichroic mirror, and LP 515 nm emission) for green-based images. With the A4 filter, callose deposits were recognized by a turquoise fluorescence and encysted zoospores by an intense, bright-blue fluorescence. With the H3 filter, plant and *P. viticola* structures were recognized by green fluorescence. The various stages of the development and structure of *P. viticola* were classified and described according to Unger *et al.* (2007) and Godard *et al.* (2009).

Staining reactive oxygen species

Leaf discs were collected before (uninoculated) and after (1 and 7 dpi) *P. viticola* inoculation and incubated in 10 µM 5-(and-6)-carboxy-2',7'-dichlorodihydrofluorescein diacetate (Invitrogen, CA, USA) for 20 min in order to stain the ROS. The leaf discs were then washed with water and microscope observations were carried out using an LMD7000 microscope mounted with an H3 filter (Leica).

Sample collection and protein extraction

For the proteomic study, leaf samples from Pinot Noir plants were collected immediately before (uninoculated) and at 1 dpi of *P. viticola*: these samples comprised T39-treated leaves (T39-uninoculated and T39-1 dpi), and controls (control-uninoculated and control-1 dpi). All the leaves from each plant were collected, then frozen in liquid nitrogen and stored at –80 °C. For each treatment, leaf samples from three replicates (plants) were collected at each time point. A total of six plants were used for each treatment, three sampled before inoculation and three at 1 dpi, in order to avoid wounding stress.

Frozen samples were ground in a mixer-mill disruptor (MM 400, Retsch, Germany) at 20 Hz for 40 s. Finely ground leaf samples were immediately suspended in 10 volumes of TCA/acetone solution (10% w/v TCA and 0.07% w/v 2-mercaptoethanol in acetone) for overnight protein precipitation at –20 °C to remove secondary metabolites. Samples were centrifuged at 17,000 *g* for 20 min at 4 °C and precipitated proteins were washed twice with three volumes of cold (–20 °C) 100% acetone, incubated at –20 °C for 2 h, and then centrifuged. To solubilize precipitated proteins, the air-dried powder was suspended in two volumes of reducing solubilization buffer (6 M urea, 2 M thiourea, 1% CHAPS, 2 mM DTT) in the presence of a protease inhibitor cocktail (1 × Complete Tablet, Roche Molecular Biochemicals, Germany) and incubated at 4 °C for 1 h with continuous shaking. The homogenate was centrifuged at 17,000 *g* for 20 min at 4 °C and solubilized proteins were stored at –80 °C. Protein concentration was determined with a protein assay (Bio-Rad, CA, USA).

Protein digestion and iTRAQ labelling

Total protein extracts (100 µg at 1 mg/ml) were denatured and reduced, and the cysteines blocked using iTRAQ reagents (8plex, AB Sciex, CA, USA), according to the manufacturer's instructions. Proteins were then diluted with five volumes of 50 mM TEAB to reduce urea concentration to 1.4 M, and twice digested with trypsin (Applied Biosystems, CA, USA) at a trypsin/protein ratio of 1:300 (37 °C, overnight. and then for 3 h). The resulting peptide solution was concentrated in a centrifugal vacuum concentrator and diluted with six volumes of 100% isopropanol.

Digested peptides were labelled with iTRAQ reagents. Samples were then mixed in equal ratios and dried in a centrifugal vacuum concentrator to remove isopropanol. Two 8-plex iTRAQ-labelled peptide mixtures were prepared. The first mixture (iTRAQ1) contained proteins extracted from control-uninoculated and control-1 dpi plants, including two technical replicates of isotopic labelling, while the second mixture (iTRAQ2) contained proteins extracted from control-uninoculated, T39-uninoculated, and T39-1 dpi plants.

Peptide clean-up and chromatography

The iTRAQ-labelled peptide mixture was cleaned using a column of ReproSil-Pur C18 AQ beads (3µm, 20Å, Dr Maisch, Germany) prepared in a 4-mm diameter syringe filter (0.2 µm, PVDF membrane, Whatman, USA). The column was equilibrated with buffer A (50% acetonitrile and 5% formic acid) and then with buffer B (5% formic acid). The iTRAQ-labelled peptide mixture was acidified with a final concentration of 5% formic acid, loaded onto the column and eluted with 100 µl buffer C (80% acetonitrile and 5% formic acid). Acetonitrile and formic acid were removed by vacuum centrifugation and cleaned samples were subject to iTRAQ-compatible OFFGEL electrophoresis (Chenau *et al.*, 2008) using an 3100 OFFGEL fractionator (Agilent Technologies, CA, USA). The iTRAQ-labelled peptide mixture was focused according to its isoelectric point on a 24-cm immobilized non-linear pH 3–10 gradient (IPG strip, Agilent Technologies), according to the manufacturer's instructions, and the default peptide-focusing programme (50 kV/h). To prevent the trapping column clogging, the 24 fractions were clarified with C18 StageTips (Thermo Scientific, Germany), as described above for the C18 AQ columns. The eluted iTRAQ-labelled peptide mixture was then vacuum-concentrated and reconstituted with 18 µl 5% formic acid.

LC-MS/MS analysis

Each fraction (5 µl) was injected into an EasyLC capillary chromatographic system (Thermo Scientific), as described in Matafora *et al.* (2009). Peptide separation was carried out using a home-made 10-cm fused silica capillary (75 µm inner diameter, 360 µm outer diameter; Thermo Scientific) filled with Reprosil-Pur C18 3 µm resin (Dr Maisch, Germany). Peptides were eluted with a 60-min gradient of eluent A (2% acetonitrile and 0.1% formic acid in distilled water) and eluent B (98% acetonitrile and 0.1% formic acid in distilled water), starting with 8% eluent B (flow rate 0.2 µl min^{-1}) and finishing with 50% (flow rate 0.2 ml min^{-1}). The EasyLC system was connected to an LTQ-Orbitrap mass spectrometer equipped with a nanoelectrospray ion source (Thermo Scientific). Full-scan mass spectra were acquired in an LTQ-Orbitrap mass spectrometer in the mass range m/z 350–1600 Da with the resolution set to 60000. The lock-mass option was used to obtain accurate mass measurements. The four most intense doubly and triply charged ions were automatically selected and fragmented in the iontrap. Target ions already selected for the MS/MS were dynamically excluded for 60 s. Target values were 1,000,000 for the survey scan and 100,000 for the MS/MS scan. Pulsed Q dissociation parameters were set at an isolation width of 3 m/z, normalized collision energy 30%, activation Q 0.55, and activation time 0.4 ms; the threshold for MS/MS acquisition was set to 200 counts. Each OFF-gel fraction was injected twice onto the LC-MS/MS (runs MS1 and MS2) to increase the number of proteins identified: a total of 96 LC-MS/MS were run.

Raw data obtained from the LC-MS/MS runs were grouped and processed using the Proteome Discoverer Software version 1.1.0 (Thermo Scientific), which uses data from the Mascot 2.2.07 search and performs relative quantification of the eight reporter ions derived from the iTRAQ reagents. The database search parameters included the following settings: number of permitted missed tryptic cleavage sites set to 2; and iTRAQ peptide labelling and confidence cut off >95%. Cysteine carbamidomethylation was searched as a fixed modification, while N-acetyl protein and oxidized methionine were searched as variable modifications. Peptide mass tolerance was set to 10 ppm and fragment mass tolerance to 0.8 Da. The criterion for evaluating the quality of the MS/MS data was an ion score cut off greater than 20. Peptides were accepted with a false discovery rate of 0.5%, estimated on the basis of the number of accepted reverse hits. Where proteins were characterized by only one peptide, this peptide had to contain at least two spectral counts and had to be classified as unique. Proteins were identified by integrating the results from two protein database searches (Supplementary Fig. S1, available at *JXB* online): the predicted Pinot Noir grapevine proteome (Release 3, http://genomics.research.iasma.it; Velasco *et al.*, 2007), and a non-redundant *Viridiplantae* Uniprot protein database (http://www.uniprot.org/taxonomy/33090, downloaded from July 2011). Due to the

size of the *Viridiplantae* Uniprot protein database, replicated LC-MS/MS runs (MS1 and MS2) were processed separately using the Proteome Discoverer Software. In order to properly quantify identified proteins, only unique peptides were subjected to protein quantification, which was calculated as the median of all peptide ratios belonging to the protein group.

Protein annotation

Additional alignments were performed to convert proteins obtained from Mascot search of the *Viridiplantae* Uniprot database into the *V. vinifera* homologue and to identify proteins not predicted from the Pinot Noir grapevine genome (Supplementary Fig. S1). An initial protein homology search was carried out against the Pinot Noir grapevine proteome with an E-value $<E^{-5}$ and identity >60%; a second search was carried out against all protein predictions of the Pinot Noir grapevine genome with an E-value $<E^{-5}$ and identity >60%; a third was carried out against the Pinot Noir grapevine genome with an E-value $<E^{-50}$ and identity >60% (Supplementary Fig. S1). Identified protein sequences were then aligned against the 12× PN40024 grapevine genome with an E-value $<E^{-20}$ (http://www.genoscope.cns.fr/externe/GenomeBrowser/Vitis; Jaillon *et al.*, 2007). Proteins obtained from Mascot search of the *Viridiplantae* Uniprot database were also aligned against the *T. atroviride* v2 (http://genome.jgi-psf.org; E-value $<E^{-50}$ and identity >60%) and *Hyaloperonospora arabidopsidis* 7.0.1 databases (http://genome.wustl.edu/genomes/view/hyaloperonospora_arabidopsidis; E-value $<E^{-50}$ and identity >60%).

Gene ontology (GO, Ashburner *et al.*, 2000) annotation was carried out by aligning the Pinot Noir grapevine proteome (Release 3) against the UniProt databases (downloaded from July 2011) using BLASTP (Altschul *et al.*, 1997). BLAST results were analysed using the ARGOT2 software (Falda *et al.*, 2012) and the associated GO biological process terms, grouped into 19 functional categories, and were used for protein annotation. The results of the automatic annotation of proteins with significant changes in abundance were manually inspected and integrated with GO biological process terms supported by evidence from the literature. GO frequencies were evaluated for proteins with significant changes in abundance compared with the Pinot Noir grapevine proteome annotations using a chi-squared test ($P < 0.05$).

For the MapMan ontology analysis (Thimm *et al.*, 2004), proteins were aligned against the *Arabidopsis thaliana* proteome TAIR9 (www.arabidopsis.org) using BLASTX with an E-value $<E^{-5}$ and identity >60%. Searches were also carried out using the Plant Protein Annotation Program (PPAP; http://www.uniprot.org/program/Plants; Schneider *et al.*, 2009) and InterProScan (http://www.ebi.ac.uk/interpro). The results of all searches were compiled and classified into MapMan BINs (http://mapman.gabipd.org). Assigned categories were then manually checked against literature searches. *Arabidopsis* MapMan pathways of overview of metabolism and photosynthesis-primary metabolisms were adopted, and a specific pathway for biotic and abiotic stresses was developed on the basis of literature searches. Proteins that could not be associated to any biological process category were assigned to the GO root (biological process) and to BIN 35.

Statistical analysis

In order to compare disease severity under the various conditions, an analysis of variance (ANOVA) was performed with the Statistica 9 software (StatSoft, OK, USA) using Tukey's test to detect significant differences between treatments ($P < 0.05$), and an F-test to identify non-significant treatment–experiment interactions ($P > 0.05$).

For the proteomic study, normalized iTRAQ ratios were $\log_2$ transformed to generate a normally distributed set of data, and processed using the Multi Experiment Viewer (MeV; http://www.tm4.org/mev/software; Saeed *et al.*, 2006). A *t* test (Welch approximation, *p*-values based on *t*-distribution, $P < 0.05$) coupled with a fold-change threshold of the log-transformed ratios was performed (volcano plot visualization). Four pairwise comparisons were performed, and the fold-change threshold was calculated as the standard deviation (δ) of log-transformed ratios, which corresponded to 0.73 for the control-1 dpi/control-uninoculated ratios, 0.74 for T39-uninoculated/control-uninoculated ratios, 0.76 for T39-1 dpi/control-uninoculated ratios, and 0.64 for T39-1 dpi/T39-uninoculated ratios.

Results

Mechanisms of disease reduction after Trichoderma harzianum T39 treatments

As previously reported (Perazzolli *et al.*, 2008), the severity of downy mildew is significantly reduced in T39-treated grapevines (Supplementary Fig. S2A). Disease reduction was also observed in T39-treated leaf discs at 7 dpi (Supplementary Fig. S2B). Specifically, sporadic sporulation (2% of incidence) was observed on T39-treated leaf discs, in contrast to intense sporulation (100% incidence) on control discs at 7 dpi. BTH was applied to grapevine plants and leaf discs, resulting in a considerable reduction of disease severity (Supplementary Fig. S2A, B).

Microscope observation of aniline blue-stained leaf discs revealed no differences between control and T39-treated plants before *P. viticola* inoculation (Fig. 1A–C). At 1 dpi, the pathogen had already penetrated the stomata of control leaf discs and encysted zoospores (Fig. 1D) and primary haustoria were visible (Fig. 1G). The number of zoospores that had successfully penetrated stomata at 1 dpi was drastically reduced in leaf discs treated with T39 (Fig. 1E, 1H) and almost completely absent in those treated with BTH (Fig. 1F, 1I). Where present, spore germination on T39-treated leaf discs was similar to controls (Fig. 1H). Strong turquoise fluorescence was observed in the stomata of BTH-treated leaf discs, indicating intense callose deposition at infection sites (Fig. 1F). A reaction in the epidermal cells surrounding *P. viticola* zoospores was also observed (Fig. 1I), indicating localized necrosis (Godard *et al.*, 2009). Turquoise fluorescence of stomatal guard cells (but not the surrounding epidermal cells) was also observed in T39-treated leaf discs (Fig. 1E, 1H), indicating early accumulation of callose. In T39-treated leaf discs, callose deposition was more localized than in BTH-treated leaf discs and there were no necrotic areas.

At 5 dpi, *P. viticola* mycelium had spread to the parenchyma of control leaves (Fig. 1J) and had produced sporangiophores at 7 dpi (Fig. 1M). In contrast, T39-treated leaf discs exhibited extensive fluorescence around the stomata at 5 dpi (Fig. 1K), indicating intense callose deposition, as in the BTH-treated leaf discs (Fig. 1L). Moreover, *P. viticola* sporulation was greatly reduced in T39-treated leaf discs (Fig. 1N) compared to control discs (Fig. 1M). Interestingly, stomata with callose deposition did not show fungal infection (Fig. 1K), suggesting that callose plays a role in T39-induced resistance to *P. viticola*. As further evidence, inhibition of callose synthesis by 2-DDG treatment negatively affected disease attenuation in T39-treated leaf discs (Fig. 1P–R). 2-DDG has been found to block callose deposition, presumably not by acting directly on the synthase but rather by affecting metabolized product (Schreiner *et al.*, 1994). Specifically, 2-DDG reduced turquoise fluorescence at 1 dpi (Supplementary Fig. S2C) and considerably increased development of *P. viticola* mycelia at 5 and 7 dpi in T39-treated leaf discs (Fig. 1Q and Supplementary Fig. S2C). A similar effect was

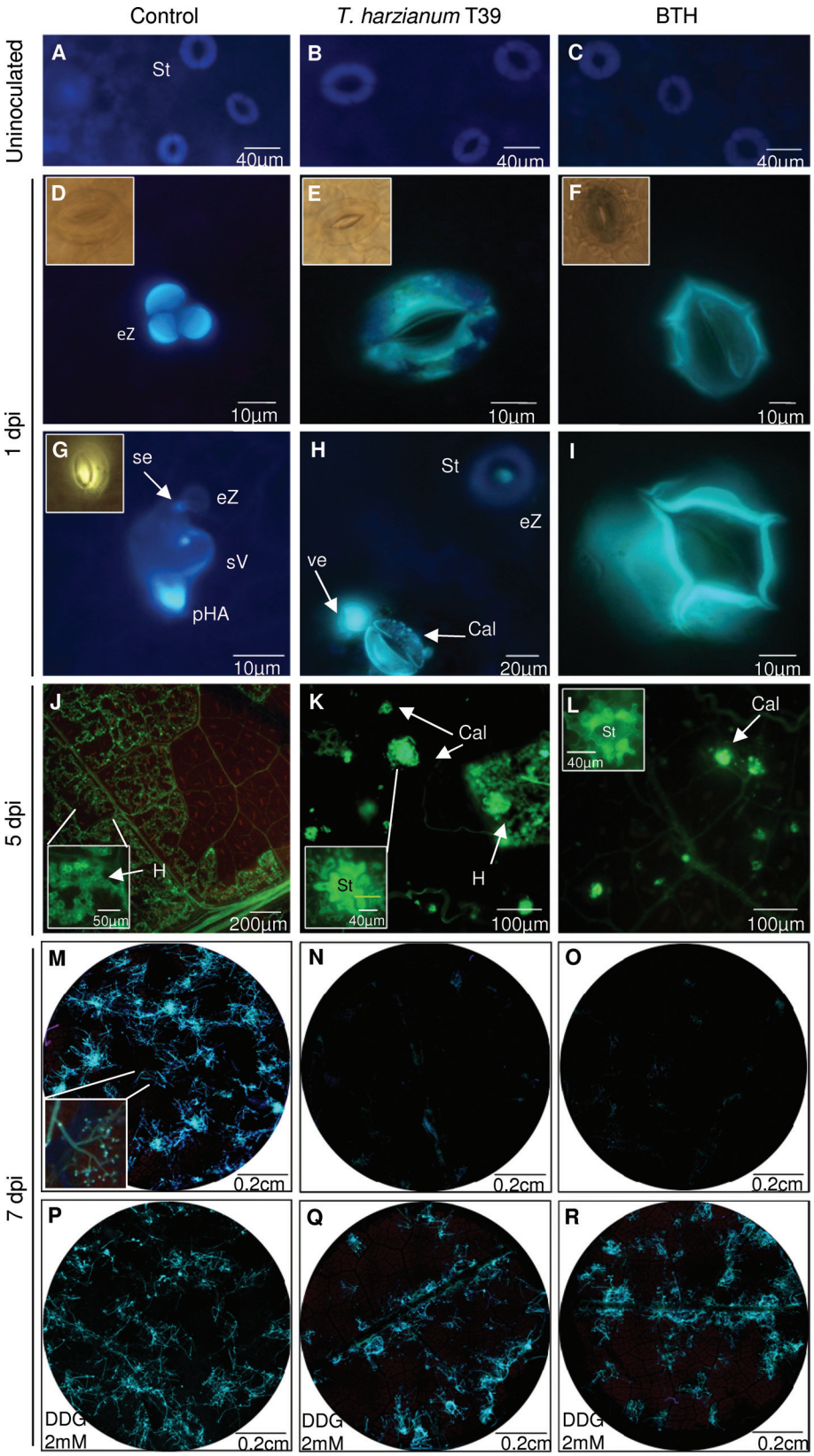

Fig. 1. Time course of intercellular colonization by *Plasmopara viticola* during *Trichoderma harzianum* T39-induced resistance. Susceptible *Vitis vinifera* cv. Pinot Noir leaf discs were treated with water (control), *T. harzianum* T39, or benzothiadiazole (BTH). Pathogen development and callose deposition were monitored before inoculation (uninoculated), and 1, 5, and 7 days post inoculation (1, 5, 7 dpi) with *P. viticola* using epifluorescence microscopy after aniline blue straining. (A–C) Uninoculated leaf discs showing basal fluorescence of stomata. (D–I) Leaf discs at 1 dpi. (D, G) Encysted zoospores on stomata and intracellular infection structures, such as a septum, between encysted zoospores, and the substomatal vesicle, were visible on control leaves at 1 dpi. (E, F, H, I) Callose deposition

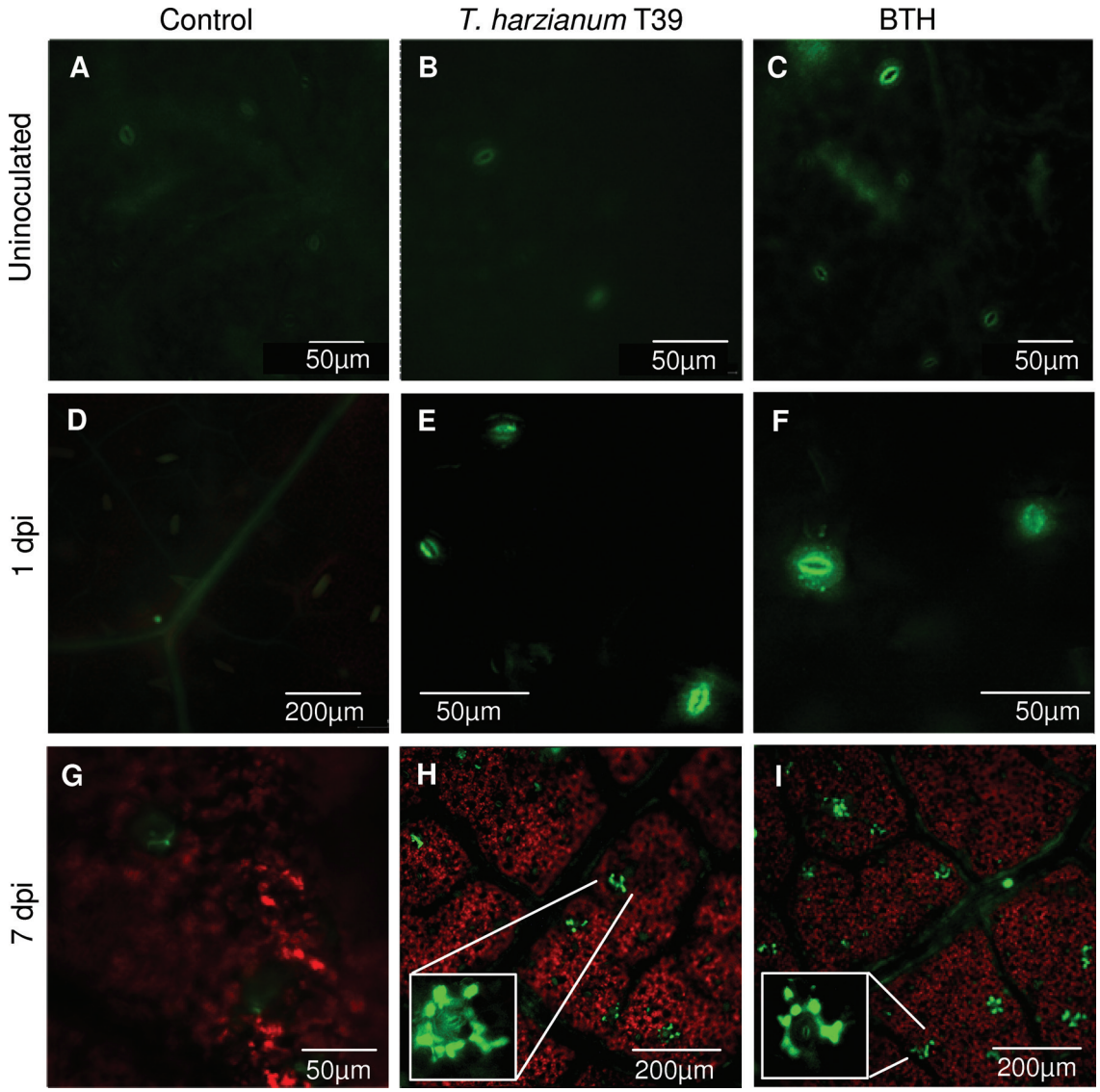

Fig. 2. Accumulation of reactive oxygen species (ROS) after *Plasmopara viticola* inoculation. Leaf discs of susceptible *Vitis vinifera* cv. Pinot Noir were treated with water (control), *Trichoderma harzianum* T39, or benzothiadiazole (BTH). ROS accumulation was monitored before inoculation (uninoculated), and 1 and 7 days post inoculation (1 and 7 dpi) with *P. viticola* using epifluorescence microscopy (Leica LMD7000, H3 filter) and 5-(and-6)-carboxy-2',7'-dichlorodihydrofluorescein diacetate fluorescent dye. (A, D, G) No fluorescence staining was visible on control leaf discs before inoculation or at 1 dpi, and only weak ROS accumulation was visible at 7 dpi in the infected area. (B, E, H) ROS were not detected on T39-treated leaf discs before inoculation; ROS accumulated in stomata cells at 1 dpi and in epidermal cells around infected stomata at 7 dpi. (C, F, I) ROS accumulation was rare on BTH-treated leaf discs before *P. viticola* inoculation but increased in the epidermal cells around the stomata between 1 and 7 dpi. Ten representative leaf discs per treatment are shown. The experiment was repeated three times with similar results.

in the stomata together with zoospores penetrating the stomata were visible on T39-treated discs (E, H), whereas only prominent callose depositions were detected on BTH-treated discs (F, I) at 1 dpi. (J–L) Leaf discs at 5 dpi. Long, branched hyphae of *P. viticola* were visible on the control (J). Intense fluorescence of epidermal cells around stomata guard cells (St) in T39-treated discs (K) and BTH-treated discs (L) indicated callose deposition. (M–R) Grapevine leaf discs after *P. viticola* sporulation (7 dpi). Sporulation was visible on the control (M), but was greatly inhibited on T39-treated discs (N) and absent from BTH-treated discs (O). Treatment with the callose synthesis inhibitor (2-DDG) reduced both T39-induced protection (Q) and BTH-induced protection (R) against *P. viticola*, sporulation being comparable to the control (P). Images were acquired by epifluorescence microscopy (Leica LMD7000) using an H3 filter for green fluorescence pictures (J–L) and an A4 filter for blue-based fluorescence pictures (A–I, M–R). A representative leaf disc of ten per treatment is shown. The experiment was repeated three times with similar results. Cal, callose deposition; eZ, encysted zoospores; H, hyphae; pHA, primary haustoria; se, septum, sV, substomatal vesicle; ve, vesicle.

observed in leaf discs treated with 2-DDG and BTH (Fig. 1R), confirming the role of callose deposition in the resistance to downy mildew.

No ROS were produced in control leaf discs before *P. viticola* inoculation and at 1 dpi (Fig. 2A, 2D) and only weak fluorescence was visible at 7 dpi around infection sites (Fig. 2G). ROS were not produced in plants treated with T39 before pathogen inoculation (Fig. 2B), but they were accumulated in guard cells at 1 dpi (Fig. 2E). The intensity of ROS fluorescence in T39-treated leaf discs increased in the days following inoculation (data not shown) and was localized in cells near the stomata (Fig. 2H). In BTH-treated leaf discs, ROS accumulation started before *P. viticola* inoculation (Fig. 2C) and it was greater than in T39-treated leaf discs after inoculation (Fig. 2F, 2I).

Optimization of the grapevine iTRAQ procedure and protein identification

In order to analyse proteomic changes associated with T39-induced resistance, leaf samples were collected from T39-treated and control plants immediately before inoculation and at 1 dpi of *P. viticola*. The latter time point was chosen in order to study early plant response, when substomatal vesicles and primary haustoria have already developed (Fig. 1D, 1G). Defence mechanisms (Fig. 1E, 1H and Fig. 2E) and defence gene induction (Perazzolli *et al.*, 2011) were also observed at 1 dpi in T39-treated grapevines. The grapevine proteome was analysed using the high-throughput eight-plex iTRAQ technique combined with a high resolution LC-MS/MS Orbitrap mass spectrometer.

Using the Pinot Noir grapevine protein database, this study identified and quantified 459 grapevine proteins in the iTRAQ1 experiment and 211 in iTRAQ2 (Table 1 and Supplementary Table S1). An additional 230 proteins were identified in iTRAQ1 and 159 in iTRAQ2 using the *Viridiplantae* Uniprot protein database, which was used to improve protein identification (Supplementary Fig. S1 and Table 1). After removing common proteins, 601 proteins were quantified in the iTRAQ1 experiment and 302 proteins were quantified in the iTRAQ2 experiment, corresponding to a total of 800 unique proteins (Table 1, Supplementary Table S1, and Supplementary Fig. S3A). Of these unique proteins, 206 were identified using the *Viridiplantae* Uniprot database (Supplementary Fig. S3B), of which 155 were homologous with one or more predicted proteins for grapevine, eight matched into the Pinot Noir grapevine genome, and 43 had no match with the Pinot Noir genome (Supplementary Fig. S1). These 43 proteins had no match even when aligned to *T. atroviride* and *H. arabidopsidis* proteomes.

Separate analyses of MS1 and MS2 were carried out with the Proteome Discoverer Software using the *Viridiplantae* Uniprot database in order to evaluate reproducibility in terms of the number of proteins commonly quantified in both MS runs: this turned out to be 22% for iTRAQ1 and 33% for iTRAQ2 (Table 1 and Supplementary Fig. S3C, D), which was similar to the rates described by other groups (Jones *et al.*, 2006; Lucker *et al.*, 2009). Having two technical replicates of isotopic labelling allowed the evaluation of the labelling efficiency. The resulting median (log transformed) of 0 and σ of 0.21 indicated the absence of a significant labelling bias between technical replicates (data not shown). The high degree of accuracy obtained with the Orbitrap mass spectrometer not only boosts confidence in protein database search results, it also shows the potential of this tool for *de novo* sequencing. Indeed, at least one *de novo* amino acid assignment was found in 52% of the total peptides quantified in iTRAQ1 and in 45% of those quantified iTRAQ2 (Table 2), leading to an improvement in grapevine proteome annotation.

Grapevine proteins with significant changes in abundance during T39-induced resistance

The global normalization protocol (summed intensities) was used to correct intensities between iTRAQ labels, and the resulting histogram of log-transformed ratios had a normal distribution (data not shown), suggesting the absence of a significant bias between samples. Statistical analysis revealed that 128 and 118 proteins had significant changes in abundance in the iTRAQ1 and iTRAQ2 experiment, respectively. These proteins were grouped into three clusters (CL) based on the different expression profiles (Fig. 3A). CL1 comprised 128 proteins affected by *P. viticola* at 1 dpi in control plants (Supplementary Table S2), CL2 comprised the 58 proteins directly affected by T39 treatment (Supplementary Table S3), and CL3 comprised the 60 proteins affected by *P. viticola* in T39-treated plants and not by T39 before pathogen inoculation (Supplementary Table S4). Interestingly, 34 proteins of CL2 were exclusively affected by T39, whereas 24 proteins were significantly affected by T39 treatment and after *P. viticola* inoculation of T39-treated plants (Supplementary Table S3). Most of the proteins in CL1 (79%)

Table 1. Proteins quantified by LC-MS/MS

Experiment	Database	Quantified proteins				Total quantified proteins
		MS1	MS2	MS1 + MS2	Total	
iTRAQ1	Pinot Noir grapevine			459	601	800
	Viridiplantae Uniprot	149	131	230		
iTRAQ2	Pinot Noir grapevine			211	302	
	Viridiplantae Uniprot	105	107	159		

In each iTRAQ experiment, two different MS runs (MS1 and MS2) and two database searches (Pinot Noir grapevine proteome and *Viridiplantae* Uniprot database) were used to maximize the number of identified proteins. After removing redundancies by a BLAST search, 601 unique proteins in iTRAQ1 and 302 in iTRAQ2 were identified. A total of 800 unique proteins were identified and quantified by Mascot search in the iTRAQ experiments.

Table 2. *De novo* peptide sequencing for improvement of the grapevine Pinot Noir proteome

Peptide sequence	Protein ID	Modifications	Peptide ion score	m/z (Da)	MH+ (Da)
XD**X**VLDFARGKGGDLIK	glimmer.VV78X173528.16_1	X1(111.0), N-Term(Acetyl), X3(111.0), K17(iTRAQ8plex)	24	724.71	2172.12
HLSTSPAG**X**SIDALSPSASSPSVR	fgenesh.VV78X255168.8_2	N-Term(iTRAQ8plex), X9(S)	24	872.46	2615.38
EDLEISSA**X**SQRTLEMEVVELRR	fgenesh.VV78X213438.7_2	N-Term(iTRAQ8plex), X9(Q), M16(Oxidation)	15	1013.50	3038.55
DFLWGGGV**X**EK	fgenesh.VV78X086249.3_3	N-Term(iTRAQ8plex), X9(P)	16	754.91	1508.82
WLPDRQMP**X**MKSLR	fgenesh.VV78X217256.7_1	N-Term(iTRAQ8plex), X9(A)	16	678.37	2033.10
FIIQMLE**X**	glimmer.VV78X175476.41_1	N-Term(iTRAQ8plex), X8(W)	16	692.38	1383.76
INGMSGL**X**R	glimmer.VV78X219975.6_1	N-Term(iTRAQ8plex), X8(T)	15	626.85	1252.69
MVGIAFD**X**ITSPSSVNSSQVPSVSPFSVYR	glimmer.VV78X147076.10_6	N-Term(iTRAQ8plex), X8(Q)	29	873.45	3490.79
DASKNWR**X**AGSDGSSQLTIK	glimmer.VV78X028231.22_4	N-Term(iTRAQ8plex), X8(N)	17	813.75	2439.25
LLVTAG**X**R	sim4.VV78X013999.4_1	N-Term(iTRAQ8plex), X7(Y)	15	399.58	1196.73
VPVSME**X**LGGIGEFFRFAIPSAVMICTR	glimmer.VV78X110157.9_11	N-Term(iTRAQ8plex), X7(W), M24(Oxidation)	16	873.45	3490.79
RREAPA**X**ALTFAEHPQMK	fgenesh.VV78X075745.12_7	N-Term(iTRAQ8plex), X7(S), M17(Oxidation)	17	787.42	2360.24
EAISLA**X**MKDEQLQR	fgenesh.VV78X252996.9_1	N-Term(iTRAQ8plex), X7(P)	15	678.37	2033.11
EVIIIS**X**R	fgenesh.VV78X017221.8_1	N-Term(iTRAQ8plex), X7(M)	29	632.88	1264.75
KDKDDL**X**SELK	twinscan.VV78X136286.3_2	N-Term(iTRAQ8plex), X7(L), K11(iTRAQ8plex)	26	638.05	1912.13
ILVIEG**X**HPMYDAR	glimmer.VV78X175632.6_4	N-Term(iTRAQ8plex), X7(L)	33	966.04	1931.07

Examples of peptides containing *de novo* amino acid assignment. In total, 1357 peptides out of 2591 in iTRAQ1 and 594 out of 1330 in iTRAQ2 contained at least one amino acid assignment. Protein ID, Accession number in the predicted Pinot Noir grapevine proteome database; Modifications, modifications identified by Mascot 2.2.07 search; m/z, peptide mass-to-charge ratio; MH+, singly protonated peptide mass.

showed a decrease in abundance, whereas this was the case for about half of the proteins in the other two clusters (45% in CL2, 46% in CL3).

Proteins were annotated and grouped into 19 selected GO biological process categories, and proteins with unknown function were assigned to the GO root (biological process; Fig. 3B). Although proteins with unknown function predominated (about 10–15%), the functional category of generation of precursor of metabolites and energy was well represented in all CLs (about 10%) compared with the grapevine proteome (2%). Moreover, in all three CLs, large groups of proteins were assigned to the functional categories of signal transduction, response to stress, and response to stimulus (more than 5, 8, and 7%, respectively). The categories of biological regulation, carbohydrate metabolic process, and nucleic acid metabolic processes (4, 8, and 4%, respectively) were significantly overrepresented in CL3 compared with the grapevine proteome.

Out of proteins with significant changes in abundance, 191 were assigned to at least one MapMan (Thimm *et al.*, 2004) functional category and the proteins with unknown function were assigned to the MapMan BIN 35. MapMan overview of metabolism and photosynthesis-primary metabolisms were used to visualize the metabolic processes affected by compatible interaction and T39-induced resistance (Supplementary Fig. S4). Visualization of proteins affected by *P. viticola* in control plants revealed global negative regulation of amino acid biosynthesis, secondary metabolism, and photosynthetic processes (Supplementary Fig. S4A). In particular, proteins involved in photosynthesis (i.e. PSII and PSI subunits and ferredoxin-NADP-oxidoreductase) and the pentose phosphate cycle (i.e. phosphoglycerate kinase and fructose-bisphosphate aldolase) had decreased abundance (Supplementary Fig. S4B). Repression of metabolic processes by *P. viticola* was attenuated during T39-induced resistance (Supplementary Fig. S4C, E). Proteins involved in amino acid metabolism (i.e. fumarylacetoacetase), cell-wall metabolism (i.e. rhamnogalacturonate lyase) and photosynthesis (i.e. photosystem I subunit D-1, a rubisco activase) had increased abundance after T39 treatment (Supplementary Fig. S4C, D). Increased abundance of proteins related to photosynthesis (i.e. chlorophyll-binding proteins, PSI and PSII subunits, ATP synthase), pentose phosphate cycle (a glyceraldehyde-3-phosphate dehydrogenase and a fructose-bisphosphate aldolase), and secondary metabolic processes (i.e. an O-acetylserine lyase, a thymidylate synthase, and a UDP-D-glucuronate 4-epimerase) was also observed after *P. viticola* inoculation in T39-treated plants (Supplementary Fig. S4E, F).

An in-house pathway of biotic and abiotic stress responses was developed in MapMan using the *Arabidopsis* biotic stress pathway as template and manually integrating it with other correlated MapMan pathways, according to information found in the literature (Fig. 4). In control plants, proteins related to receptor classes (two LRR receptor-like proteins, cysteine-rich receptor-like protein kinase, and a G-type lectin S-receptor-like serine/threonine-protein kinase) had mostly decreased abundance, whereas proteins related to signal cascade [two recognition of *Peronospora parasitica* (RPP) proteins and three nucleotide-binding site-encoding resistance (NBS-R) proteins] had increased abundance at 1 dpi (Fig. 4A), indicating weak recognition of *P. viticola*. Interestingly,

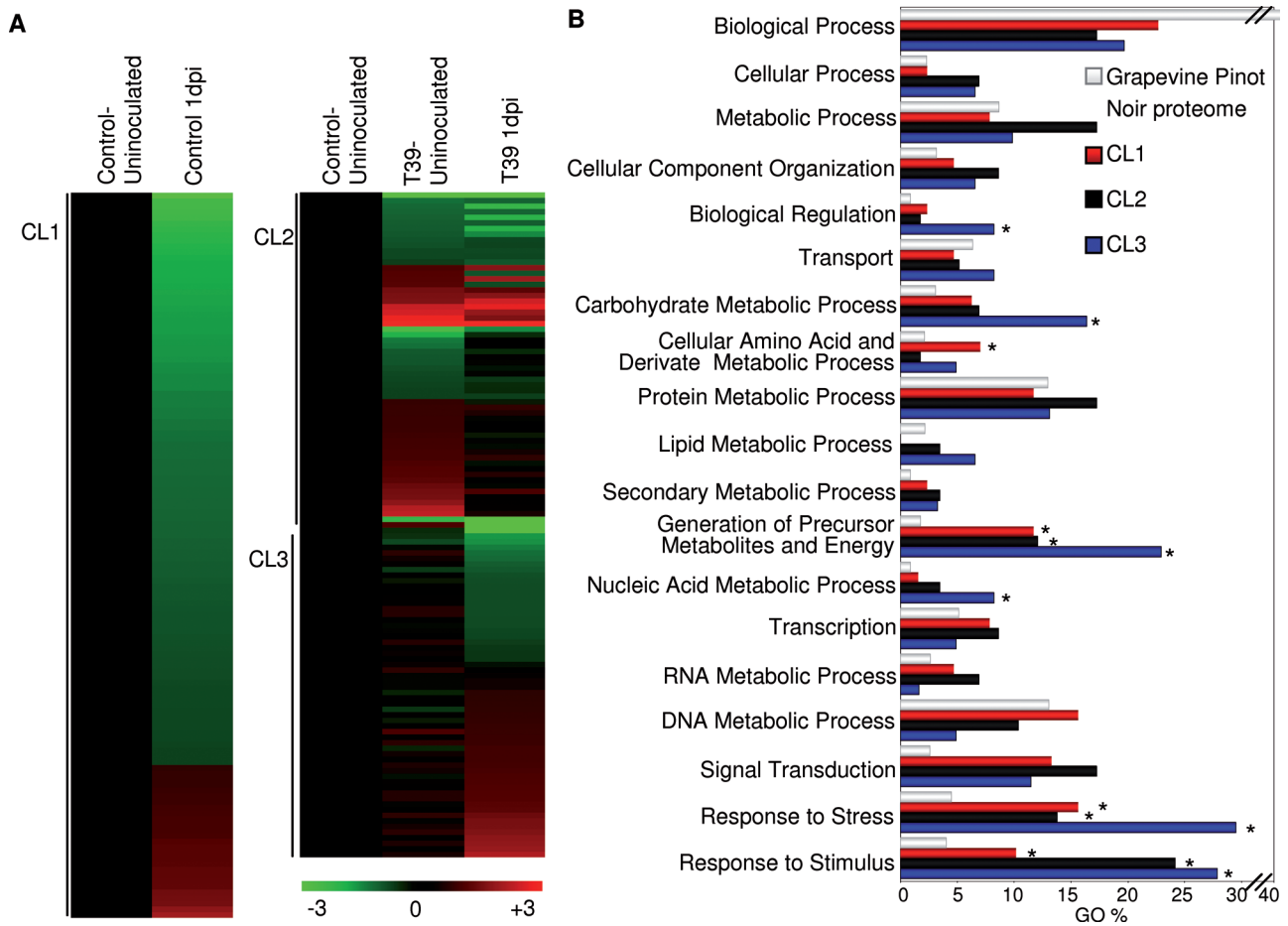

Fig. 3. Clustering and gene ontology (GO) annotation of proteins with significant changes in abundance during T39-induced resistance. (A) Proteins were grouped in clusters (CLs) according to their expression profiles: CL1, proteins significantly affected by *Plasmopara viticola* at 1 dpi in control plants (n = 128); CL2, proteins significantly affected by *Trichoderma harzianum* T39 treatment (n = 58); CL3, proteins significantly affected by *P. viticola* at 1 dpi in T39 plants (n = 60), according to comparisons control-uninoculated vs. T39-1dpi, and T39-uninoculated vs. T39-1dpi. Proteins of CL2 were either exclusively affected by T39 (34 proteins) or affected by T39 and by *P. viticola* in T39-treated plants (24 proteins). (B) Distribution of significantly affected proteins across 19 GO functional categories. GO frequencies were calculated as percentages of the total number of biological process terms (195 in CL1, 107 in CL2, and 131 in CL3, and 39,399 in the total Pinot Noir grapevine proteome). For each CL, categories marked by an asterisk were differentially represented to the total Pinot Noir grapevine proteome, according to a chi-squared test ($P < 0.05$).

P. viticola inoculation mostly decreased the abundance of proteins involved in transport, transcription regulation, and signal transduction pathways, such as ethylene (ET)-, jasmanic acid (JA)- and SA-mediated signalling in control plants. On the other hand, proteins involved in biotic and abiotic stress response had increased abundance in T39-treated plants (Fig. 4B). T39 treatment caused an increase in abundance of two receptors (a leucine-rich repeat receptor-like protein kinase and a receptor-like protein kinase precursor), a guanine nucleotide-binding protein (GTPase-activating protein), three resistance proteins (an RPP protein and two TMV resistance proteins N), proteins involved in hormone signalling (abscisic acid and auxin signalling and metabolism), and redox balance (a thioredoxin and a ferredoxin-thioredoxin reductase). In addition, other proteins associated with signal transduction (a *Pseudomonas syringae* resistant protein, a Rabgap/TBC domain-containing protein, and two disease resistance proteins) and redox balance (a glutaredoxin, a copper/zinc superoxide dismutase, and a glutathione reductase) were induced in T39-treated plants after *P. viticola* inoculation, showing that control and T39-treated plants react differently to pathogen infection.

Discussion

Trichoderma species have been recognized as biocontrol agents for a number of pathogens (Perazzolli *et al.*, 2008; Vinale *et al.*, 2008; Shoresh *et al.*, 2010). The biocontrol ability of *Trichoderma* species is based on different mechanisms, such as antibiosis, mycoparasitism, competition, and induction of plant resistance (Shoresh *et al.*, 2010). In grapevine, the T39 strain reduces downy mildew severity by activating plant-mediated

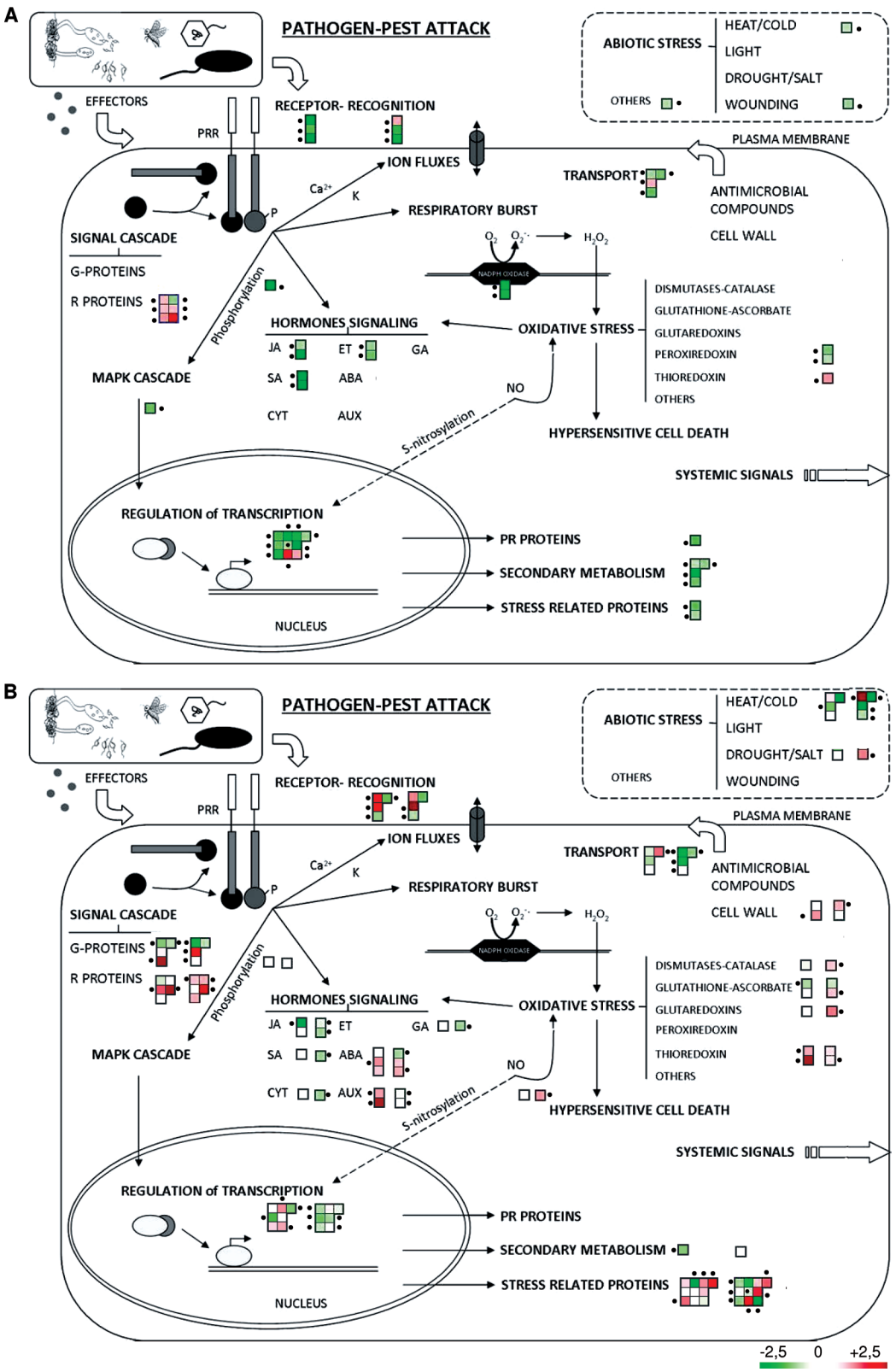

Fig. 4. Biotic and abiotic stress responses. MapMan overview of proteins with significant changes in abundance during *Trichoderma harzianum* T39-induced resistance. The pathway was originally generated from information in the literature and pre-existing MapMan pathways. Annotation of proteins was manually checked and the assigned BINs were loaded onto MapMan software. Each square represents a significantly affected protein (green, decreased in abundance; red, increased in abundance) compared with control-uninoculated plants. (A) Proteins significantly affected by *Plasmopara viticola* inoculation in control plants (CL1). (B) Proteins significantly affected in T39-treated plants. Expression levels before (squares on the left of each BIN) and after (squares on the right) *P. viticola* inoculation in T39-treated plants are shown. Asterisks indicate the pairwise comparisons with significant change in protein abundance.

resistance mechanisms, without any direct toxic effect on *P. viticola* sporangia germination (Perazzolli *et al.*, 2008). T39-induced resistance is mediated by direct modulation of defence-related genes and by their enhanced expression after pathogen inoculation (Perazzolli *et al.*, 2011). Whereas direct antagonistic effects of T39 could occur at the early stages of zoospores germination, pronounced accumulation of callose in stomata guard cells was observed at 1 dpi in T39-treated plants. The present histological analysis indicates that biocontrol mechanisms of T39-induced resistance are related to the early activation of plant defence processes, which begin as soon as the zoospore germ tubes have penetrated the stomata and mainly involve plugging and closure of stomata. Moreover, high amounts of ROS were produced in stomata guard cells in T39-treated plants at 1 dpi of *P. viticola*. Interestingly, *P. viticola* was never observed in the areas of ROS accumulation, suggesting a prominent role of ROS in the T39-induced resistance to downy mildew. As reported for other inducers (Trouvelot *et al.*, 2008; Allegre *et al.*, 2009), the biochemical changes in T39-treated grapevines mainly occurred subsequent to downy mildew inoculation. This response indicates that T39 primes grapevine defences, as suggested by the absence of apparent energy costs in T39-treated plants (Perazzolli *et al.*, 2011).

In order to better understand the cellular processes associated with the early stages of T39-induced resistance, proteomic changes activated by T39 were analysed before and at 1 dpi of *P. viticola*. The high-throughput eight-plex iTRAQ protocol combined with an integrated approach to protein identification, resulted in the quantification of 800 unique proteins. Of these, 43 proteins did not match with Pinot Noir, or the *T. atroviride* and *H. arabidopsidis* proteomes, indicating that the analysis had identified grapevine proteins not yet predicted by bioinformatic approaches or proteins belonging to natural microorganisms of the leaf phyllosphere. Interestingly, about half the total quantified peptides contained at least one *de novo* amino acid assignment in their sequence, which will be used to improve annotation of the Pinot Noir protein sequences.

Annotation of the proteins with significant changes in abundance highlighted considerable differences in the responses of T39-treated and control plants to *P. viticola* inoculation. Interestingly, 58 proteins were directly affected by T39 treatment (CL2) and 60 proteins were affected after pathogen inoculation in T39-treated plants (CL3), confirming the dual effect of T39 previously suggested by gene expression analyses (Perazzolli *et al.*, 2011).

Grapevine proteins affected by Plasmopara viticola *in control plants*

Analysis of the grapevine proteome in response to *P. viticola* infection revealed weak pathogen recognition coupled with an ineffective attempt to activate a resistance response at 1 dpi (CL1). Proteins responsible for microbial recognition and signal transduction components (for example, five NBS-R proteins) increased in abundance at 1 dpi. In particular, changes in abundance of two proteins similar to the *Arabidopsis* recognition of *Peronospora parasitica* (RPP8), known to be induced by oomycete infection (McDowell *et al.*, 1998), suggested recognition of *P. viticola*. However, the increase in abundance of these proteins did not correspond to an effective activation of resistance response in grapevine. The lack of a downstream defence response could be interpreted as being part of a pathogen defence suppression strategy (Milli *et al.*, 2011). Indeed, suppression of endogenous signalling pathways by pathogenic effectors is probably required to establish compatible interactions (Milli *et al.*, 2011) and is followed by metabolic reprogramming associated with compatibility (Polesani *et al.*, 2008, 2010). Suppression of defence responses is corroborated by the repression of grapevine proteins involved in signal transduction processes at 1 dpi (i.e. a RAF-like MAP3Ks involved in ET-mediated signalling and the homologue of resistance-inducing protein PBS1). Similarly, proteins associated with hormone metabolism and hormone signalling were found to be less abundant after *P. viticola* inoculation: for example, a 1-aminocyclopropane-1-carboxylate synthase, a lipoxygenase (LOX), a RRM-containing protein, polyubiquitin 10, and a PKN/PRK1 effector-like domain protein. Among the proteins whose abundance was decreased, two NADPH-oxidases, a peroxiredoxin 2B and a peroxiredoxin Q (Prx Q), involved in controlling redox balance. In particular, *PrxQ* has been reported to be repressed by *P. viticola* at the oil spot stage (Polesani *et al.*, 2008).

Proteins associated with defence (a defence response-induced protein), responses to abiotic stresses (a heat shock protein DNAJ homologue), and secondary metabolism (two polyphenol oxidase, a flavonoid 3'-monooxygenase, and a momilactone A synthase-like) had decreased abundance in control plants at 1 dpi.

Among the proteins related to transport, a vacuolar ATP synthase and a voltage-dependent anion channel (VDAC) had decreased abundance. VDAC proteins are porin-type β-barrel diffusion pores and are involved in the formation of permeability transition pores (PTP; Shimizu *et al.*, 2001), which can contribute to cell shrinkage during the hypersensitive response (Kusano *et al.*, 2009). Since obligate biotrophic fungi require living host cells to complete their infection cycle, the decrease in abundance of VDCA could be part of the attempt by *P. viticola* to keep the host alive.

P. viticola inoculation mainly caused a decrease in abundance of proteins involved in photosynthesis (PSII D2 proteins, PSI subunit F and D1, ferredoxin-NADP-oxidoreductase 1 and 2), pentose phosphate cycle (aldolase, GAP, FBPase, phosphoglycerate kinase, and PRK) and photorespiration (glycine decarboxylase P-protein 1 and 2). A decrease in abundance of proteins related to photosynthetic processes has been previously observed during *P. viticola* infection (Milli *et al.*, 2011) and linked to source-to-sink transition of infected tissues (Gamm *et al.*, 2011).

Grapevine proteins directly affected *by T39*

T39 treatment directly affected proteins (CL2) associated with signal transduction, response to stresses, response to stimuli and energy metabolism. As part of signal transduction, ten proteins were directly affected by T39 and eight of them maintained similar expression levels after *P. viticola* inoculation, indicating that the microbial recognition machinery is active prior to pathogen arrival and may create the conditions for a rapid

response. Among the receptor-recognition proteins, a probable LRR-kinase, a receptor-like protein kinase, and three NBS-R proteins (two TMV resistance proteins N and RPP8) increased in abundance, in agreement with *Trichoderma*-treated maize and bean (Marra *et al.*, 2006; Shoresh and Harman, 2008). Moreover, three proteins of the G protein family were affected by T39. In particular, a GTPase-activating protein, AGD3-like, a key regulator of vesicular trafficking of auxin efflux in *Arabidopsis* (Sieburth *et al.*, 2006), increased in abundance, suggesting that vesicle trafficking processes are involved in the *Trichoderma*-induced response.

Among the stress related proteins, T39 increased the abundance of a member of the non-specific lipid transfer protein (nsLTP) family. Genes encoding LTPs were induced by *Trichoderma* spp. in cacao and *Arabidopsis* plants (Bailey *et al.*, 2006; Morán-Diez *et al.*, 2012) and several LTPs showed antimicrobial properties (Blein *et al.*, 2002). Interestingly, a nsLTP (glimmer.VV78X270940.4_1) increased in abundance after T39 treatment (CL2), and another nsLTP isoform (glimmer.VV78X102158.67_1) increased in abundance upon *P. viticola* inoculation of T39-treated plants (CL3), indicating specific involvement of LTP isoforms in plant responses.

T39 affected two proteins involved in the thioredoxin system: a chloroplast thioredoxin (TRX) M-type and a ferrodoxin-dependent TRX reductase (FTR). TRXs play a role in redox regulation of enzyme activities (Gelhaye *et al.*, 2005), suggesting that they could be components of the signalling pathways in the T39-induced plant antioxidant network.

Regarding hormone metabolism and signalling, a marker for the JA pathway (LOX protein) displayed a decrease in abundance upon T39 treatment. JA has been implicated in T39-induced resistance in *Arabidopsis* (Korolev *et al.*, 2008) and resistance to *P. viticola* in resistant (Polesani *et al.*, 2010) or elicited (Hamiduzzaman *et al.*, 2005; Trouvelot *et al.*, 2008; Perazzolli *et al.*, 2011) grapevines. Induction by T39 followed by enhanced expression after *P. viticola* inoculation of T39-treated plants has been observed in LOX9 at the transcriptional level (Perazzolli *et al.*, 2011), indicating specific involvement of LOX isoforms in grapevine response.

A direct correlation between the ability of *Trichoderma* spp. to promote plant growth and its ability to induce proteins associated with carbohydrate metabolism has been reported for *T. harzianum* T22 in maize (Shoresh and Harman, 2008) and for *T. hamatum* 382 in tomato (Alfano *et al.*, 2007). This is backed up by the correlation between absence of an increase in abundance of proteins associated with carbohydrate metabolism and the lack of growth benefits observed in T39-treated grapevines (Perazzolli *et al.*, 2011).

Grapevine proteins affected by Plasmopara viticola *in T39-treated plants*

When *Trichoderma*-treated plants were challenged with a pathogen, defence gene expression and protective enzyme activity were enhanced compared with inoculated control plants (Perazzolli *et al.*, 2011; Brotman *et al.*, 2012). The current results show that proteins affected by *P. viticola* in T39-treated plants (CL3) are mainly associated with response to stress, photosynthesis, redox signalling, and energy metabolism. Proteins associated with photosynthesis and energy metabolism mostly increased in abundance in T39-treated plants in response to *P. viticola*, highlighting a specific reaction of plants treated with the resistance inducer. A correlation between increased level of proteins involved in photosynthesis and respiration and increased level of enzymes associated with cell-wall expansion has been observed in a maize–*Trichoderma* interaction (Shoresh and Harman, 2008). An UDP-D-glucuronate 4-epimerase responsible for pectin biosynthesis (Usadel *et al.*, 2004) showed an increase in abundance in T39 at 1 dpi, indicating that cell-wall synthesis is activated after *P. viticola* inoculation. Defence-related reinforcement of cell walls in T39-treated plants was also evidenced by callose deposition around stomata at 1 and 5 dpi and by the restoration of *P. viticola* development following 2-DDG treatment. Further support for the role of callose deposition and ROS accumulation in T39-treated plants was the induction of a Rab-GAP/TBC domain-containing protein. Rab-GAP proteins are key regulators of intracellular vesicular trafficking for the apposition of papillae components at the site of oomycete penetration (Novick and Zerial, 1997; Collinge, 2009).

Interestingly, no receptor kinases were found in CL3 but they were directly affected by T39 treatment (CL2), suggesting that the microbial recognition machinery is pre-activated by T39 in preparation for a rapid response upon pathogen arrival. Among the proteins associated with signal transduction, this study identified three resistance proteins that increased in abundance upon *P. viticola* inoculation in T39 treated plants. Of these, the homologous protein resistant to *Pseudomonas syringae* 5 has been associated with resistance to *Peronospora parasitica* and *Pseudomonas syringae* in *Arabidopsis*, suggesting the existence of a common protein that may be required for multiple resistance protein signal cascades (Warren *et al.*, 1998).

Among the proteins associated with oxidative stress, a glutathione reductase, a copper/zinc superoxide dismutase (SOD), and a glutaredoxin had increased abundance in T39-treated plants after *P. viticola* inoculation. Alteration of oxidative stress metabolism is consistent with ROS accumulation observed in T39 treated plants at 1 and 7 dpi of *P. viticola*. SODs are responsible for converting superoxide anion to hydrogen peroxide and their activation during *T. harzianum*-induced redox reprogramming have been related to the resistance in sunflower (Singh *et al.*, 2011). These results suggest that the concentration of oxidizing species induced upon *P. viticola* inoculation is kept under control by an array of enzymes in T39-treated plants in order to avoid biological damage.

Proteins involved in JA/ET signalling were identified in CL3, consistent with the finding that these pathways are involved in T39-induced resistance (Korolev *et al.*, 2008; Perazzolli *et al.*, 2008). In particular, *P. viticola* caused a decrease in abundance of an activation domain protein in T39-treated plants. Together with the protein kinases MEKK1 and WRKY53, the activation domain protein mediates negative cross-talk between defence and senescence processes, which are governed by JA and SA equilibrium (Miao and Zentgraf, 2007). Another protein involved in the ET signal cascade was a putative

ubiquitin-conjugating enzyme (De Paepe *et al*., 2004), which had increased abundance after *P. viticola* inoculation of T39-treated plants. The expression profiles of the activation domain protein, UBC, and the LOX of CL2 evidenced cross-communication between SA and JA/ET pathways during T39-induced resistance. As already reported, *Trichoderma*–plant cross-talk is dynamic and regulation of JA/ET and SA pathways may be essential for an efficient defence mechanism (Hermosa *et al*., 2012). Thus, in the *Trichoderma*–grapevine interaction, cross-talk between hormone pathways could help the plant to minimize energy costs and to create a flexible signalling network to fine-tune defence response to invaders.

Conclusions

This study assessed the proteomic and histochemical changes associated with *Trichoderma*-induced resistance, before and after pathogen inoculation. In addition to biological information, the high-throughput proteome analysis and the integrated use of two protein databases resulted in identification of 51 grapevine proteins not yet predicted by bioinformatic approaches, and in improvement in peptide sequences by *de novo* sequencing. Identification of proteins with significant changes in abundance provides molecular markers of grapevine induced resistance and highlights key processes that might further studied to improve T39-induced resistance against downy mildew. Major future challenges will be to validate the roles of individual proteins and explore their function in regulatory mechanisms responsible for T39-induced resistance.

Supplementary material

Supplementary data are available at *JXB* online.

Supplementary Table S1. Proteins identified and quantified in control-uninoculated and control-1dpi plants in the iTRAQ1 experiment and in control-uninoculated, *Trichoderma harzianum* T39-uninoculated, and *T. harzianum* T39-1 dpi plants in the iTRAQ2.

Supplementary Table S2. Proteins affected by *Plasmopara viticola* inoculation in control plants (CL1).

Supplementary Table S3. Proteins affected by *Trichoderma harzianum* T39 treatment (CL2).

Supplementary Table S4. Proteins affected by *Plasmopara viticola* inoculation in *Trichoderma harzianum* T39-treated plants (CL3).

Supplementary Fig. S1. Annotation of quantified proteins.

Supplementary Fig. S2. *Trichoderma harzianum* T39-induced resistance in susceptible *Vitis vinifera* cv. Pinot Noir.

Supplementary Fig. S3. Proteins commonly quantified in different iTRAQ experiments.

Supplementary Fig. S4. MapMan metabolic overview and photosynthesis-primary pathways.

Acknowledgements

This research was supported by the Accordo di programma, the EnviroChange and the Post-Doc Project 2006 Resistevite projects funded by the Autonomous Province of Trento. The authors thank Yigal Elad (The Volcani Center, Israel) for producing the *T. harzianum* T39 (Trichodex), Oscar Giovannini (Fondazione Edmund Mach) for his help in the experiments under greenhouse conditions and Emanuele Alpi (San Raffaele Scientific Institute) for his help with the Proteome Discoverer Software.

References

Alfano G, Ivey MLL, Cakir C, Bos JIB, Miller SA, Madden LV, Kamoun S, Hoitink HAJ. 2007. Systemic modulation of gene expression in tomato by *Trichoderma hamatum* 382. *Phytopathology* **97,** 429–437.

Allegre M, Heloir MC, Trouvelot S, Daire X, Pugin A, Wendehenne D, Adrian M. 2009. Are grapevine stomata involved in the elicitor-induced protection against downy mildew? *Molecular Plant–Microbe Interactions* **22,** 977–986.

Altschul SF, Madden TL, Schaffer AA, Zhang J, Zhang Z, Miller W, Lipman DJ. 1997. Gapped BLAST and PSI-BLAST: a new generation of protein database search programs. *Nucleic Acids Research* **25,** 3389–3402.

Ashburner M, Ball CA, Blake JA, *et al.* 2000. Gene ontology: tool for the unification of biology. *Nature Genetics* **25,** 25–29.

Bailey B, Bae H, Strem M, Roberts D, Thomas S, Crozier J, Samuels G, Choi I-Y, Holmes K. 2006. Fungal and plant gene expression during the colonization of cacao seedlings by endophytic isolates of four *Trichoderma* species. *Planta* **224,** 1449–1464.

Bayles CJ, Ghemawat MS, Aist JR. 1990. Inhibition by 2-deoxy-d-glucose of callose formation, papilla deposition, and resistance to powdery mildew in an ml-o barley mutant. *Physiological and Molecular Plant Pathology* **36,** 63–72.

Blein J-P, Coutos-Thévenot P, Marion D, Ponchet M. 2002. From elicitins to lipid-transfer proteins: a new insight in cell signalling involved in plant defence mechanisms. *Trends in Plant Science* **7,** 293–296.

Brotman Y, Lisec J, Méret M, Chet I, Willmitzer L, Viterbo A. 2012. Transcript and metabolite analysis of the *Trichoderma*-induced systemic resistance response to *Pseudomonas syringae* in *Arabidopsis thaliana*. *Microbiology* **158,** 139–146.

Chenau J, Michelland S, Sidibe J, Seve M. 2008. Peptides OFFGEL electrophoresis: a suitable pre-analytical step for complex eukaryotic samples fractionation compatible with quantitative iTRAQ labeling. *Proteome Science* **6,** 9.

Collinge DB. 2009. Cell wall appositions: the first line of defence. *Journal of Experimental Botany* **60,** 351–352.

De Paepe A, Vuylsteke M, Van Hummelen P, Zabeau M, Van Der Straeten D. 2004. Transcriptional profiling by cDNA-AFLP and microarray analysis reveals novel insights into the early response to ethylene in *Arabidopsis*. *The Plant Journal* **39,** 537–559.

Díez-Navajas AM, Greif C, Poutaraud A, Merdinoglu D. 2007. Two simplified fluorescent staining techniques to observe infection structures of the oomycete *Plasmopara viticola* in grapevine leaf tissues. *Micron* **38,** 680–683.

Díez-Navajas AM, Wiedemann-Merdinoglu S, Greif C, Merdinoglu D. 2008. Nonhost versus host resistance to the grapevine downy mildew, *Plasmopara viticola*, studied at the tissue level. *Phytopathology* **98,** 776–780.

Di Gaspero G, Cipriani G, Adam-Blondon AF, Testolin R. 2007. Linkage maps of grapevine displaying the chromosomal locations of 420 microsatellite markers and 82 markers for R-gene candidates. *Theoretical and Applied Genetics* **114,** 1249–1263.

EPPO. 2001. Guidelines for the efficacy evaluation of fungicides: *Plasmopara viticola*. *EPPO Bulletin* **31,** 313–317.

Falda M, Toppo S, Pescarolo A, Lavezzo E, Di Camillo B, Facchinetti A, Cilia E, Velasco R, Fontana P. 2012. Argot2: a large scale function prediction tool relying on semantic similarity of weighted Gene Ontology terms. *BMC Bioinformatics* **13,** S14.

Gamm M, Héloir M-C, Bligny R, *et al.* 2011. Changes in carbohydrate metabolism in *Plasmopara viticola*-infected grapevine leaves. *Molecular Plant–Microbe Interactions* **24,** 1061–1073.

Gelhaye E, Rouhier N, Navrot N, Jacquot JP. 2005. The plant thioredoxin system. *Cellular and Molecular Life Sciences* **62,** 24–35.

Gessler C, Pertot I, Perazzolli M. 2011. *Plasmopara viticola*, the causal agent of downy mildew of grapes. *Phytopathologia Mediterranea* **50,** 3–44.

Godard S, Slacanin I, Viret O, Gindro K. 2009. Induction of defence mechanisms in grapevine leaves by emodin- and anthraquinone-rich plant extracts and their conferred resistance to downy mildew. *Plant Physiology and Biochemistry* **47,** 827–837.

Hamiduzzaman MM, Jakab G, Barnavon L, Neuhaus J-M, Mauch-Mani B. 2005. β-Aminobutyric acid-induced resistance against downy mildew in grapevine acts through the potentiation of callose formation and jasmonic acid signaling. *Molecular Plant–Microbe Interactions* **18,** 819–829.

Hermosa R, Viterbo A, Chet I, Monte E. 2012. Plant-beneficial effects of *Trichoderma* and of its genes. *Microbiology* **158,** 17–25.

Jaillon O, Aury J-M, Noel B, *et al.* 2007. The grapevine genome sequence suggests ancestral hexaploidization in major angiosperm phyla. *Nature* **449,** 463–467.

Jones AME, Bennett MH, Mansfield JW, Grant M. 2006. Analysis of the defence phosphoproteome of *Arabidopsis thaliana* using differential mass tagging. *Proteomics* **6,** 4155–4165.

Jürges G, Kassemeyer HH, Durrenberger M, Duggelin M, Nick P. 2009. The mode of interaction between *Vitis* and *Plasmopara viticola* Berk. & Curt. Ex de Bary depends on the host species. *Plant Biology* **11,** 886–898.

Korolev N, Rav David D, Elad Y. 2008. The role of phytohormones in basal resistance and *Trichoderma*-induced systemic resistance to *Botrytis cinerea* in *Arabidopsis thaliana*. *BioControl* **53,** 667–683.

Kortekamp A. 2006. Expression analysis of defence-related genes in grapevine leaves after inoculation with a host and a non-host pathogen. *Plant Physiology and Biochemistry* **44,** 58–67.

Kusano T, Tateda C, Berberich T, Takahashi Y. 2009. Voltage-dependent anion channels: their roles in plant defense and cell death. *Plant Cell Reports* **28,** 1301–1308.

Lucker J, Laszczak M, Smith D, Lund S. 2009. Generation of a predicted protein database from EST data and application to iTRAQ analyses in grape (*Vitis vinifera* cv. Cabernet Sauvignon) berries at ripening initiation. *BMC Genomics* **10**, 50.

Marra R, Ambrosino P, Carbone V, *et al.* 2006. Study of the three-way interaction between *Trichoderma atroviride*, plant and fungal pathogens by using a proteomic approach. *Current Genetics* **50,** 307–321.

Matafora V, D'Amato A, Mori S, Blasi F, Bachi A. 2009. Proteomics analysis of nucleolar SUMO-1 target proteins upon proteasome inhibition. *Molecular and Cellular Proteomics* **8,** 2243–2255.

McDowell JM, Dhandaydham M, Long TA, Aarts MGM, Goff S, Holub EB, Dangl JL. 1998. Intragenic recombination and diversifying selection contribute to the evolution of downy mildew resistance at the RPP8 locus of *Arabidopsis*. *The Plant Cell* **10,** 1861–1874.

Miao Y, Zentgraf U. 2007. The antagonist function of *Arabidopsis* WRKY53 and ESR/ESP in leaf senescence is modulated by the jasmonic and salicylic acid equilibrium. *The Plant Cell* **19,** 819–830.

Milli A, Cecconi D, Bortesi L, *et al.* 2011. Proteomic analysis of the compatible interaction between *Vitis vinifera* and *Plasmopara viticola*. *Journal of Proteomics*. **75,** 1284–1302.

Morán-Diez E, Rubio B, Domínguez S, Hermosa R, Monte E, Nicolás C. 2012. Transcriptomic response of *Arabidopsis thaliana* after 24 h incubation with the biocontrol fungus *Trichoderma harzianum*. *Journal of Plant Physiology* **169,** 614–620.

Novick P, Zerial M. 1997. The diversity of Rab proteins in vesicle transport. *Current Opinion in Cell Biology* **9,** 496–504.

Perazzolli M, Dagostin S, Ferrari A, Elad Y, Pertot I. 2008. Induction of systemic resistance against *Plasmopara viticola* in grapevine by *Trichoderma harzianum* T39 and benzothiadiazole. *Biological Control* **47,** 228–234.

Perazzolli M, Roatti B, Bozza E, Pertot I. 2011. *Trichoderma harzianum* T39 induces resistance against downy mildew by priming for defense without costs for grapevine. *Biological Control* **58,** 74–82.

Polesani M, Bortesi L, Ferrarini A, *et al.* 2010. General and species-specific transcriptional responses to downy mildew infection in a susceptible (*Vitis vinifera*) and a resistant (*V. riparia*) grapevine species. *BMC Genomics* **11,** 117.

Polesani M, Desario F, Ferrarini A, Zamboni A, Pezzotti M, Kortekamp A, Polverari A. 2008. cDNA-AFLP analysis of plant and pathogen genes expressed in grapevine infected with *Plasmopara viticola*. *BMC Genomics* **9,** 142.

Saeed AI, Bhagabati NK, Braisted JC, *et al.* 2006. TM4 microarray software suite. *Methods in Enzymology* **411,** 134–193.

Sánchez Márquez S, Bills GF, Zabalgogeazcoa I. 2007. The endophytic mycobiota of the grass *Dactylis glomerata*. *Fungal Diversity* **27,** 171–195.

Schneider M, Lane L, Boutet E, Lieberherr D, Tognolli M, Bougueleret L, Bairoch A. 2009. The UniProtKB/Swiss-Prot knowledgebase and its Plant Proteome Annotation Program. *Journal of Proteomics* **72,** 567–573.

Schreiner KA, Hoddinott J, Taylor GJ. 1994. Aluminum-induced deposition of (1,3)-β-glucans (callose) in *Triticum aestivum* L. *Plant and Soil* **162,** 273–280.

Segarra G, Casanova E, Bellido D, Odena MA, Oliveira E, Trillas I. 2007. Proteome, salicylic acid, and jasmonic acid changes in cucumber plants inoculated with *Trichoderma asperellum* strain T34. *Proteomics* **7,** 3943–3952.

Shimizu S, Matsuoka Y, Shinohara Y, Yoneda Y, Tsujimoto Y. 2001. Essential role of voltage-dependent anion channel in various forms of apoptosis in mammalian cells. *The Journal of Cell Biology* **152,** 237–250.

Shoresh M, Harman GE. 2008. The molecular basis of shoot responses of maize seedlings to *Trichoderma harzianum* T22 inoculation of the root: a proteomic approach. *Plant Physiology* **147,** 2147–2163.

Shoresh M, Harman GE, Mastouri F. 2010. Induced systemic resistance and plant responses to fungal biocontrol agents. *Annual Review of Phytopathology* **48,** 21–43.

Sieburth LE, Muday GK, King EJ, Benton G, Kim S, Metcalf KE, Meyers L, Seamen E, Van Norman JM. 2006. SCARFACE encodes an ARF-GAP that is required for normal auxin efflux and vein patterning in *Arabidopsis*. *The Plant Cell* **18,** 1396–1411.

Singh B, Singh A, Singh S, Singh H. 2011. *Trichoderma harzianum*-mediated reprogramming of oxidative stress response in root apoplast of sunflower enhances defence against *Rhizoctonia solani*. *European Journal of Plant Pathology* **131,** 121–134.

Thimm O, Bläsing O, Gibon Y, *et al.* 2004. Mapman: a user-driven tool to display genomics data sets onto diagrams of metabolic pathways and other biological processes. *The Plant Journal* **37,** 914–939.

Trouvelot S, Varnier AL, Allègre M, *et al.* 2008. A β-1,3 glucan sulfate induces resistance in grapevine against *Plasmopara viticola* through priming of defense responses, including HR-like cell death. *Molecular Plant–Microbe Interactions* **21,** 232–243.

Unger S, Buche C, Boso S, Kassemeyer HH. 2007. The course of colonization of two different *Vitis* genotypes by *Plasmopara viticola* indicates compatible and incompatible host-pathogen interactions. *Phytopathology* **97,** 780–786.

Usadel B, Schlüter U, Mølhøj M, Gipmans M, Verma R, Kossmann J, Reiter W-D, Pauly M. 2004. Identification and characterization of a UDP-d-glucuronate 4-epimerase in *Arabidopsis*. *FEBS Letters* **569,** 327–331.

Van Hulten M, Ton J, Pieterse CMJ, Van Wees SCM. 2010. Plant defense signaling from the underground primes aboveground defenses to confer enhanced resistance in a cost-efficient manner. In: F Baluška, V Ninkovic, eds, *Plant communication from an ecological perspective*. Berlin, Heidelberg: Springer, pp 43–60.

Velasco R, Zharkikh A, Troggio M, *et al.* 2007. A high quality draft consensus sequence of the genome of a heterozygous grapevine variety. *PLoS ONE* **2,** e1326.

Vinale F, Sivasithamparam K, Ghisalberti EL, Marra R, Woo SL, Lorito M. 2008. *Trichoderma*–plant–pathogen interactions. *Soil Biology and Biochemistry* **40,** 1–10.

Warren RF, Henk A, Mowery P, Holub E, Innes RW. 1998. A mutation within the leucine-rich repeat domain of the *Arabidopsis* disease resistance gene RPS5 partially suppresses multiple bacterial and downy mildew resistance genes. *The Plant Cell* **10,** 1439–1452.